Concurrent Relay-PID Control for Motor Position Servo Systems

Guomin Li and Kai Ming Tsang*

Abstract: A Concurrent Relay-PID controller (CRPID) for motor position servo systems is proposed in this paper. The proposed controller is composed of a deadband-relay subcontroller and a parallel PID subcontroller. The deadband-relay subcontroller is capable of improving the transient system performance while the PID subcontroller is responsible for near steady state system regulation. Systematic design methods for various controller components are developed. Design procedures are illustrated by an example. The proposed hybrid scheme is applied to a DC motor position servo system. Both numerical and experimental results demonstrate that the proposed controller performs satisfactorily and is superior to PID control alone.

Keywords: Motor control, nonlinear control, PID, relay control, servo systems.

1. INTRODUCTION

Electrical motor servo systems are indispensable in modern industries. For example, they are widely used in robotics, electrical vehicles and automated factories. Although many advanced control techniques such as self-tuning control [1], model reference adaptive control [2], sliding mode control [3] and fuzzy control [4] have been proposed to improve system performances, the conventional PI/PID controllers are still dominant in majority of real-world servo systems [5,6].

PID controllers are simple in structure and easy for implementation. However, they may produce large overshoots and over-oscillatory responses. Combining PID control with other control techniques often results in advanced hybrid schemes that are able to improve pure PID controllers. For example, Kim et al proposed a fuzzy pre-compensated PID controller for a DC motor position servo system [7]; Matsunaga et al presented a switching-type hybrid scheme in which the system controller switches between a fuzzy controller and a PID controller [8]; Li et al developed a concurrent Fuzzy Logic-PI controller using genetic algorithms [9].

Manuscript received April 21, 2006; revised March 19, 2007; accepted March 26, 2007. Recommended by Editorial Board member Dong Hwan Kim under the direction of Editor Jae Weon Choi. The support of The Hong Kong Polytechnic University for the conduct of the research is greatly acknowledged.

Guomin Li is with Axiomatic Technologies Corp., Toronto, Ontario, Canada (e-mail: guominli@ieee.org).

Kai Ming Tsang is with Department of Electrical Engineering, The Hong Kong Polytechnic University, Hung Hom, Kowloon, Hong Kong (e-mail: steve.tsang@polyu.edu.hk).

* Corresponding author.

This paper proposes a Concurrent Relay-PID controller (CRPID) for motor position servo systems. The proposed CRPID is composed of a deadband-relay subcontroller and a parallel PID subcontroller. The deadband-relay subcontroller is capable of improving transient system performance while the PID subcontroller is mainly responsible for steady state system performance.

Relay control [10] can be regarded as a special type of variable structure control. It has an attractive feature of fast response. However, relay control is often accompanied by limit cycle oscillations [11]. The proposed CRPID uses a deadband relay to eliminate these oscillations. Therefore, the developed hybrid controller has the advantages of both PID and relay controls, but at the same time eliminates limit cycle oscillations.

The paper is organized as follows. Section 2 describes the proposed control scheme. Section 3 addresses design methodologies for two subcontrollers. Section 4 illustrates design procedures for an example system and explores feasibility of the proposed scheme numerically. Section 5 applies the proposed CRPID to a real DC motor position servo system and discusses experimental results. A method to reduce control chattering resulting from high frequency noises is also addressed in this section. Both numerical and experimental results demonstrate that the proposed CRPID greatly improves the transient performance of the tested motor position servo system. This is concluded in Section 6.

2. CONTROL SCHEME

Fig. 1 shows a block diagram of the proposed Concurrent Relay-PID controller (CRPID). Two subcontrollers are included in the scheme. The PID subcontroller is an ordinary PID controller. The

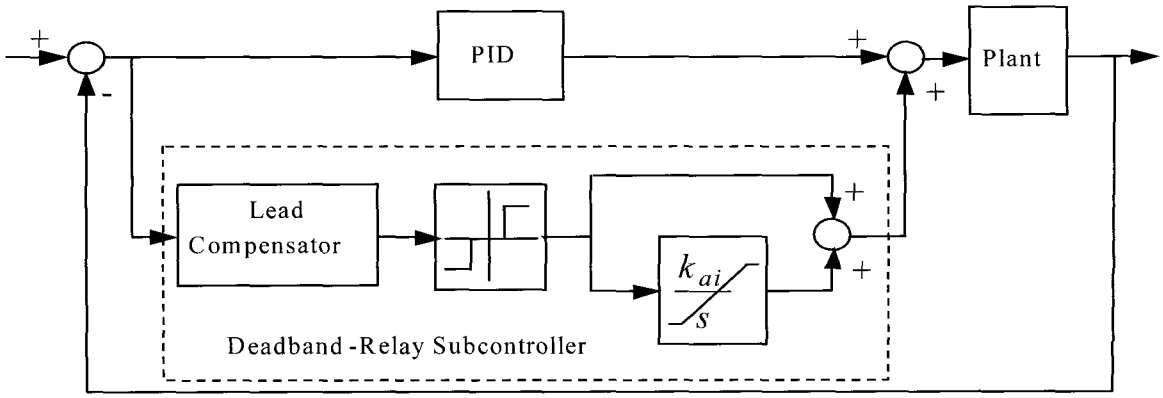

Fig. 1. Scheme of Concurrent Relay-PID controller (CRPID).

deadband-relay subcontroller is composed of a deadband relay, an auxiliary limited integrator, and a lead compensator. The deadband relay [12,13] is a relay with a deadband of certain threshold around zero input. The output of the deadband relay is either the positive or negative maximum controller output, if its input is beyond the dead band, or zero, if its input is within the dead band.

When the system has a large error, the deadband-relay subcontroller instantly outputs a control signal of either the positive or negative maximum value, so that the system responds quickly and error decreases rapidly. The deadband-relay subcontroller maintains its output until the system error becomes small enough. After that time, the deadband-relay subcontroller is automatically turned off due to the characteristics of the deadband, and the PID subcontroller alone handles the system regulation around the steady state.

The auxiliary limited integrator is to assist the PID subcontroller with near-steady-state regulation. Due to the fast response of the deadband-relay subcontroller in the transient state, the integrator in the PID subcontroller may not accumulate sufficient strength to maintain the system output after the deadband-relay subcontroller switches off. If the auxiliary limited integrator is not included, the settling time may therefore become longer. The limited integrator accumulates errors in the initial transient state only, and stops accumulation immediately after the deadband-relay subcontroller is turned off. Hence, the limited integrator actually provides an initial value for the system regulation near the steady state where only the PID subcontroller is in effect.

There are often unavoidable modeling errors when a model of the plant is developed. The lead compensator is therefore included to increase the relative stability of the resultant closed-loop system.

3. DESIGN METHODOLOGY

3.1. Design of PID subcontroller

Since the overall controller turns into PID subcontroller alone after the system error falls into and remains within the deadband of the relay, the design of the PID subcontroller is independent of that of the deadband-relay subcontroller. That is, the PID subcontroller can be designed as if only a single PID controller were employed in the system.

The methods for designing PID controllers for electrical motor speed/position servo systems have actually been well established. These methods can be classified into two main categories: "theoretical design methods" and "engineering design methods". The former include general root locus design method and various frequency-domain design methods. The latter are usually based on engineering simplification and/or reduction of plant models, utilization of pole-zero cancellation techniques, and employment of approximate design formulae for standard type 1 or type 2 systems. The Ziegler-Nichols limit cycle tuning method [14] mainly for process controls may also be used to design PID controllers for motor servo systems, and it can be regarded as an engineering design method.

It should be pointed out that the proposed CRPID is initially intended to improve the transient performance of PID control. That is, it is often implied that a PID controller has already been designed. Hence, this pre-obtained PID controller may naturally be used as the PID subcontroller in the proposed scheme.

3.2. Design of deadband relay

Fig. 2 shows the input-output characteristics of a deadband relay, where d denotes the relay output amplitude, h represents the threshold, x is the input, and z is the output.

The describing function of the deadband relay can be derived as [12,13]

$$N(X)=\frac{4d}{\pi X}\sqrt{1-(\frac{h}{X})^2}, \tag{1}$$

where

$N(X)$: describing function of the deadband relay,
X : sinusoidal input amplitude of the deadband relay,
d : relay output amplitude,
h : half of the dead band width.

The describing function of the deadband relay is a real quantity, because in its derivation there is no phase shift between the sinusoidal input and the fundamental component of the output.

In the describing function analysis of nonlinear systems, the inverse of the describing function is employed [15]. The inverse of the above describing function is denoted by

$$\frac{1}{N(X)} = \frac{\pi X}{4d\sqrt{1-(\frac{h}{X})^2}}. \tag{2}$$

The inverse of the deadband relay describing function is not a monotonic function of X. It has a minimum value at some point in the admissible set of X: $\{X \mid X > h\}$.

The point for the inverse to take its minimum value can be found as

$$X = \sqrt{2}\,h. \tag{3}$$

The minimum value of the inverse is

$$[\frac{1}{N(X)}]_{\min} = \frac{\pi h}{2d}. \tag{4}$$

It is known that the $-\frac{1}{N(X)}$ locus is employed for the stability analysis of the control system. Unlike the basic relay and the relay with hysteresis [15], the $-\frac{1}{N(X)}$ locus of the deadband relay does not go to the origin or anywhere on the imaginary axis, because of the nonzero minimum value of the inverse of the describing function. That is, there is a gap between the $-\frac{1}{N(X)}$ locus and the imaginary axis on the Nyquist plane. It is this gap that makes it possible to eliminate limit cycle oscillations in the closed-loop system with a deadband relay [12,13].

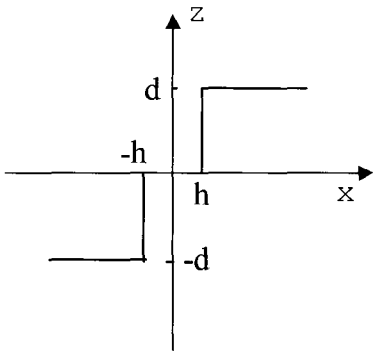

Fig. 2. Input-output characteristics of a deadband relay.

Usually, the relay output amplitude is selected to be the allowable maximum control input applied to the plant (which is very often the saturation value of the controller output), in order to fully utilize the bang-bang control property of the relay. The gap of the $-\frac{1}{N(X)}$ locus of the relay away from the imaginary axis, $[\frac{1}{N(X)}]_{\min}$, is thereby uniquely dependent on the threshold of the relay. A larger threshold leads to a more stable system but results in a less effective deadband-relay subcontroller. If the threshold is too large, the deadband-relay subcontroller may never take effect. Therefore, the selection of the threshold must satisfy

$$0 < h < |e|_{\max}, \tag{5}$$

where

$|e|_{\max}$: maximum absolute error.

Clearly, the maximum absolute error is varying in general. Only in the case of a step reference input, its value is straightforward and simply equal to the set-point value of the input. In tracking control systems, the determination of the maximum system error can be much harder. Therefore, extra efforts may be needed. Where rigorous analytical estimation is not easy, numerical study or trial-and-error will be required to assist with this task. The cardinal rule is that in order for the deadband-relay subcontroller to take as much effect as possible, the threshold of the relay is required to be as small as possible. A future direction of the study would be to explore adaptive threshold methods.

3.3. Design of limited integrator

The objective of the limited integrator, following the deadband relay, is to help reducing the settling time of the transient response of the system. The input of the limited integrator is either a train of pulses whose amplitudes are positive or negative relay output amplitude, in large-error transients, or zero after the deadband relay switches off. The larger the relay output amplitude is, the faster the limited integrator integrates. In order for the limited integrator to have an appropriate final value, which is supposed to have nothing to do with the relay output amplitude (but varies as the reference input changes), the gain of the limited integrator should be inversely proportional to the relay output amplitude.

The limited integrator is to complement the integrator already embedded in the PID subcontroller for fast settling-down of the system. Hence, the gain

of the limited integrator should be in some way related to the integral gain of the PID subcontroller.

Based on the above analysis plus a lot of numerical studies, the determination of the gain of the limited integrator is empirically suggested as

$$k_{ai} = \frac{6k_i}{d}, \tag{6}$$

where

k_{ai} : gain of the limited integrator,

k_i : integral gain of the PID subcontroller.

To avoid excessive overshoots in case of large changes of set-point values, an integral anti-windup must be employed. This can be done by simply stopping the integration of the limited integrator when its output reaches a certain level (e.g., 50%) of the allowed maximum controller output.

The limited integrator may alternatively be designed together with the lead compensator within a more rigorous and systematic framework, such as by means of root locus method. However, that will make the design more sophisticated. Therefore, (6) is very useful for the separated design of the limited integrator, although it was developed empirically. The later simulation and experimental results will demonstrate the effectiveness of this empirical formula.

It must be pointed out that diligence is always required in determining the gain of the limited integrator, since an excessively large gain could adversely affect the settling time of the entire system.

3.4. Design of lead compensator

The lead compensator is to improve the relative stability of the closed-loop system. Since both the small threshold of the deadband relay and the integration of the auxiliary limited integrator tend to deteriorate the system stability, the lead compensator in the deadband-relay subcontroller is very important.

The deadband relay can be represented by its describing function if all high frequency harmonics are attenuated effectively in the closed-loop system. Fig. 3(a) shows a block diagram of the closed-loop system in terms of transfer functions/describing function, where $G_c(s)$ denotes the transfer function of the PID subcontroller, $G_l(s)$ stands for the transfer function of the lead compensator, $G_p(s)$ is the transfer function of the plant, and $G_{pi}(s)$ is the transfer function of the pseudo-PI controller following the deadband relay, which is given by

$$G_{pi}(s) = \frac{s + k_{ai}}{s}. \tag{7}$$

The characteristic equation of the closed-loop system is

$$1 + [G_l \cdot N(X) \cdot G_{pi} + G_c]G_p = 0 \tag{8}$$

or

$$\frac{G_l G_{pi} G_p}{1 + G_c G_p} = -\frac{1}{N(X)}. \tag{9}$$

For the closed-loop system to be stable, the $-\frac{1}{N(X)}$ locus must be away from the locus of the transfer function $\frac{G_l G_{pi} G_p}{1 + G_c G_p}$ on the Nyquist plane. Hence, the inclusion of the lead compensator is actually to modify the locus of $\frac{G_l G_{pi} G_p}{1 + G_c G_p}$ in an appropriate way so that the closed-loop system is not only absolutely stable but also with a good relative stability.

In a minimum-phase system, the $-\frac{1}{N(X)}$ locus is actually characterized by its right end point, i.e., point $(-[\frac{1}{N(X)}]_{\min}, j0)$, only [12,13]. Hence, designing a lead compensator for the deadband-relay subcontroller is equivalent to designing a lead compensator for a plant denoted by $\frac{G_{pi} G_p}{1 + G_c G_p}$ with the $(-[\frac{1}{N(X)}]_{\min}, j0)$ point rather than the (-1, j0) point as the critical point.

The phase margin of the closed-loop system is given by

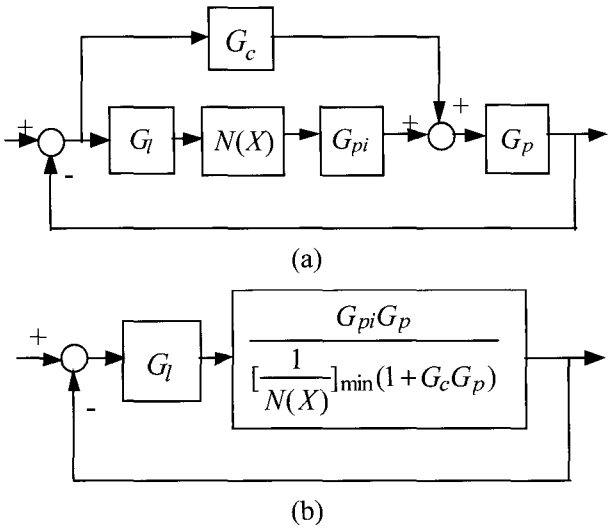

Fig. 3. (a) Block diagram of the closed-loop system (b) Equivalent system for the design of lead compensator.

$$\gamma = \angle \frac{G_l G_{pi} G_p(j\varpi_{cg})}{1 + G_c G_p(j\varpi_{cg})} + 180^\circ \tag{10}$$

equivalently,

$$\gamma = \angle \frac{G_l G_{pi} G_p(j\varpi_{cg})}{[\frac{1}{N(X)}]_{\min}[1 + G_c G_p(j\varpi_{cg})]} + 180^\circ, \tag{11}$$

where γ is the phase margin and ϖ_{cg} is the gain crossover frequency satisfying

$$\left| \frac{G_l G_{pi} G_p(j\varpi_{cg})}{1 + G_c G_p(j\varpi_{cg})} \right| = [\frac{1}{N(X)}]_{\min} \tag{12}$$

equivalently,

$$\left| \frac{G_l G_{pi} G_p(j\varpi_{cg})}{[\frac{1}{N(X)}]_{\min}[1 + G_c G_p(j\varpi_{cg})]} \right| = 1. \tag{13}$$

The gain margin of the closed-loop system is given by

$$K_g = \frac{[\frac{1}{N(X)}]_{\min}}{\left| \frac{G_l G_{pi} G_p(j\varpi_{cp})}{1 + G_c G_p(j\varpi_{cp})} \right|} = \frac{1}{\left| \frac{G_l G_{pi} G_p(j\varpi_{cp})}{[\frac{1}{N(X)}]_{\min}[1 + G_c G_p(j\varpi_{cp})]} \right|}, \tag{14}$$

where K_g is the gain margin and ϖ_{cp} is the phase crossover frequency satisfying

$$\angle \frac{G_l G_{pi} G_p(j\varpi_{cp})}{1 + G_c G_p(j\varpi_{cp})} = -180^\circ \tag{15}$$

equivalently,

$$\angle \frac{G_l G_{pi} G_p(j\varpi_{cp})}{[\frac{1}{N(X)}]_{\min}[1 + G_c G_p(j\varpi_{cp})]} = -180^\circ. \tag{16}$$

Therefore, designing a lead compensator for the deadband-relay subcontroller is equivalent to designing a lead compensator for a plant with the transfer function of $\frac{G_{pi} G_p}{[\frac{1}{N(X)}]_{\min}(1 + G_c G_p)}$ in the conventional sense.

Fig. 3(b) shows the equivalent system for the design of lead compensator. To design the lead compensator for the deadband-relay subcontroller is thereby converted into an ordinary system compensation problem. Therefore, any readily available design tools such as MATLAB Toolboxes can be immediately employed.

4. NUMERICAL INVESTIGATION

Suppose the controlled plant is represented by

$$G_p(s) = \frac{18.3}{s(0.1s + 1)}. \tag{17}$$

This is actually a model of a laboratory motor position servo system to be discussed in the next section. Assume the positive/negative maximum control signal is -2.2/2.2 (volts), which also corresponds to the real case of the experimental system.

A PID controller for the above plant has been designed [12]. It is characterized by

$$G_c(s) = 0.85 + \frac{2.83}{s} + 0.057s. \tag{18}$$

Since the absolute maximum controller output is equal to 2.2 (volts), the output amplitude of the deadband relay is set to 2.2 (volts). Select the threshold of the deadband relay as 0.15. The two parameters of the deadband relay are then determined as

$$d = 2.2,$$
$$h = 0.15.$$

According to (4), the minimum value of the inverse of the describing function for the deadband relay is computed as

$$[\frac{1}{N(X)}]_{\min} = \frac{\pi \times 0.15}{2 \times 2.2} = 0.107. \tag{19}$$

From (6), the gain of the limited integrator is determined as

$$k_{ai} = \frac{6 \times 2.83}{2.2} = 7.718. \tag{20}$$

The anti-windup limits of the auxiliary integrator are selected to be ±1.1 volts (half of the maximum and minimum outputs of the controller).

The relative stability of the equivalent system shown in Fig. 3(b) can easily be evaluated by means of Control System Toolbox on the platform of MATLAB.

The open-loop transfer function of the uncompensated equivalent system is

$$\frac{G_{pi}G_p}{[\frac{1}{N(X)}]_{\min}(1+G_cG_p)} = \frac{171.03s+1320}{0.1s^3+2.043s^2+15.555s+51.79}. \quad (21)$$

The gain margin and phase margin of the equivalent system without a lead compensator can then be computed as

$$\gamma = 17.7^\circ,$$
$$K_g = \infty.$$

Clearly, the relative stability of the uncompensated system is poor due to a small phase margin.

A lead compensator with a unit static gain is often of the form

$$G_l(s) = \frac{Ts+1}{\alpha Ts+1} (0 < \alpha < 1), \quad (22)$$

where

T : time constant of the numerator,

α : ratio of the time constants.

Using Bode-Diagram based frequency design method, the lead compensator is designed as

$$G_l(s) = \frac{0.05s+1}{0.005s+1}. \quad (23)$$

The open-loop transfer function of the compensated equivalent system is then

$$\frac{G_lG_{pi}G_p}{[\frac{1}{N(X)}]_{\min}(1+G_cG_p)} = \frac{8.551s^2+237s+1320}{0.0005s^4+0.1102s^3+2.121s^2+15.81s+51.79}. \quad (24)$$

The gain margin and phase margin can then be evaluated as

$$\gamma = 63^\circ,$$
$$K_g = \infty.$$

The relative stability of the closed-loop system has been greatly improved.

The proposed scheme is simulated using SIMULINK Toolbox with MATLAB. The amplitude constraints imposed on the two subcontrollers as well as on the overall hybrid controller are emulated by adding appropriate saturation elements. The same anti-windup method is applied to the PID subcontroller. The simulation period is selected to be 0.001s.

Fig. 4 gives both the system response and the overall control signal waveform in the case of a step reference input. It can be seen that the system response is quick and the overshoot is less than 10%. Also, the control chattering disappears after the error falls within the pre-selected threshold.

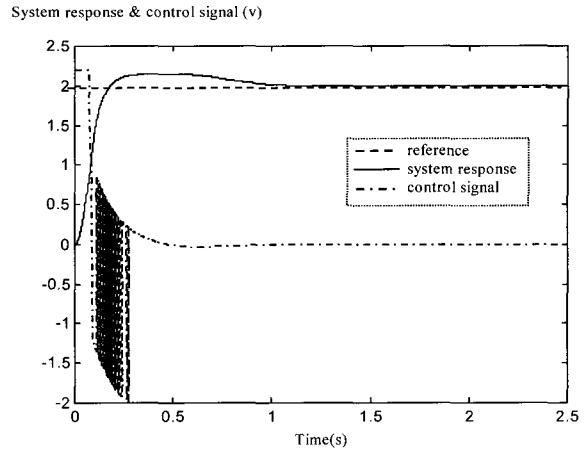

Fig. 4. Simulated step response and control signal.

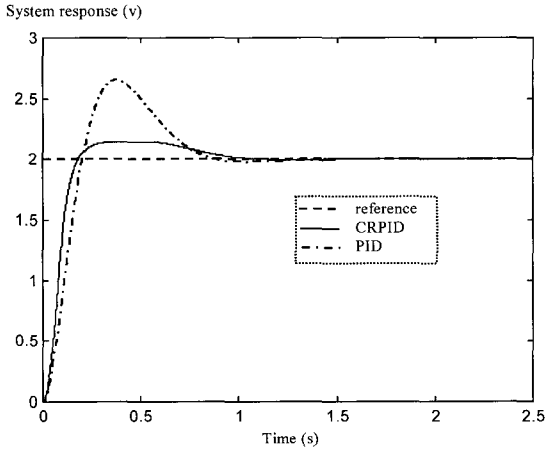

Fig. 5. Simulated system responses for CRPID and PID alone.

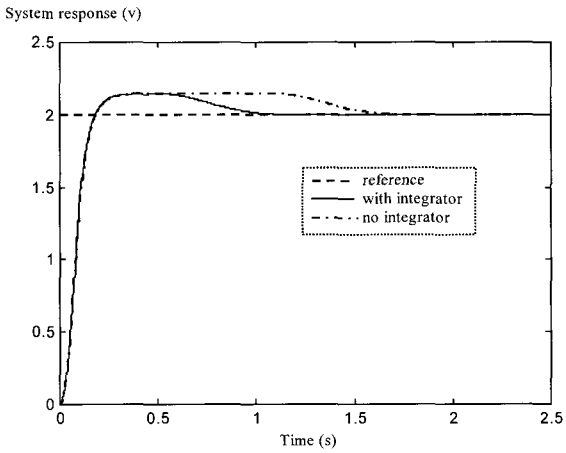

Fig. 6. Step responses of the system with and without limited integrator.

Fig. 5 is a comparison of CRPID with PID alone.

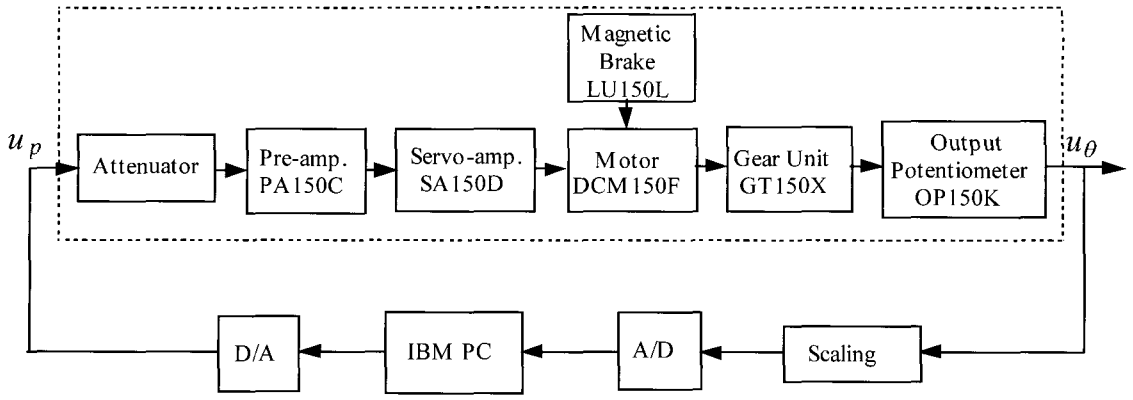

Fig. 7. Block diagram of the experimental setup.

CRPID yields a much better transient response characterized by a much smaller overshoot and a faster rise time.

Fig. 6 shows step responses of the system with and without auxiliary limited integrator. It can be seen that the auxiliary limited integrator greatly speeds up the settling-time of the system.

5. EXPERIMENTAL STUDY

The proposed CRPID is applied to a laboratory scale DC motor position servo system to verify its effectiveness. Fig. 7 is a block diagram of the experimental setup. The controlled plant in the dotted box consists of a voltage attenuator, a pre-amplifier, a servo amplifier, a permanent magnet DC motor, a gear reduction unit, a position transducer (output potentiometer) and a magnetic brake. Except for the voltage attenuator, the rest are standard modules selected from MS150 modular servo system that is supplied by Feedback Company and dedicated for laboratory experimentation. Plant output u_θ denotes the actual output shaft position expressed in voltage measured from the position transducer. Plant input u_p is the control voltage generated by the controller.

The servo amplifier SA150D is a power amplifier with a double-ended input and a double-ended output. It must be used together with the pre-amplifier PA150C to convert a single-ended input into a double-ended output. An experimental test shows that the effective input of the pre-amplifier is -0.22~0.22 volts. If the input to the pre-amplifier is beyond this range, the combination of the pre-amplifier and the servo amplifier will be saturated. The voltage attenuator with a gain of 0.1 is therefore designed to increase the allowable voltage level of the plant input for more accurate signal processing. Hence, the maximum effective input voltage of the attenuator, i.e., the maximum value of the plant input is 2.2 volts.

IBM PC undertakes such tasks as reference generation, data acquisition, real-time control, data recording and system monitoring. The A/D and D/A conversions are completed with the help of a dedicated Plug-in DT2811 conversion board provided by Data Translation. The control program is written in C++ and run in a stand-alone (non-Windows) real time mode.

A model of the plant has been developed as [12].

$$G_p(s) = \frac{18.3}{s(0.1s+1)} \tag{25}$$

The controller parameters for this experimental system modeled above were actually already determined in the last section. It is noted that the derivative in the developed PID subcontroller is replaced by an approximate derivative with a low-pass filter. The sampling time is selected to be 0.001s as was in simulation.

Fig. 8 shows a step response of the experimental system employing the proposed CRPID controller. The position response is expressed in voltage, which is measured from the position transducer, as already mentioned. To experimentally compare CRPID with PID, the experimental response for PID control alone is also given in the same figure. It can be seen that the proposed CRPID performs well and it is superior to

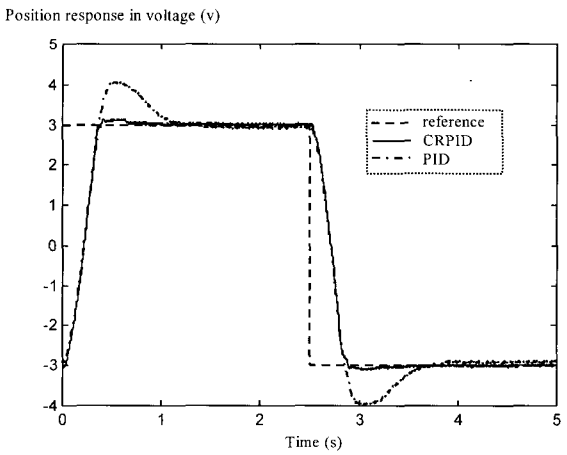

Fig. 8. Experimental step responses for CRPID and PID alone.

the PID control alone. Note that both control schemes have the same rise time in the case of large-amplitude step reference input, because the PID controller also yields a maximum control signal at the beginning of regulation, due to the integral saturation.

Fig. 9 exhibits both the experimental response of the system and the actual control signal. Different from the simulated result, the actual control signal includes a lot of high frequency chattering. This chattering is caused by high frequency noises unavoidable in the experimental system.

Although the above control chattering did not cause any harmful effects in the discussed experimental system, it may produce undesirable mechanical noises in systems of large power capacities. Hence, it is necessary to search for methods to suppress such control chattering.

A lead compensator is actually a high-pass filter. The lead compensator of (23) has a gain of 10 for high frequency components. Any unavoidable noises in the experimental system are thereby magnified by 10 times as well. This magnification should be removed in order to suppress control chattering.

Since lag compensator has a property of high frequency attenuation, it is possible to reduce control chattering by introducing a lag compensator to the deadband-relay subcontroller. In order that the inclusion of a lag compensator does not affect the system stability, the corner frequencies of the lag compensator are required to be sufficiently larger than the corner frequencies of the existent lead compensator.

The transfer function of the designed lag compensator is given by

$$\frac{0.0003s+1}{0.003s+1}. \tag{26}$$

This lag compensator attenuates high frequency components by 10 times.

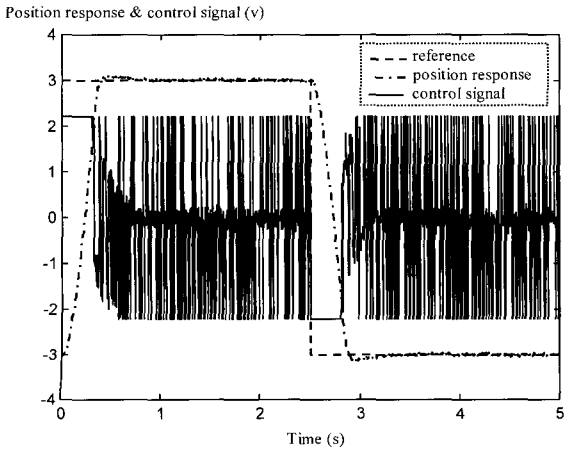

Fig. 9. Experimental position response and actual control signal.

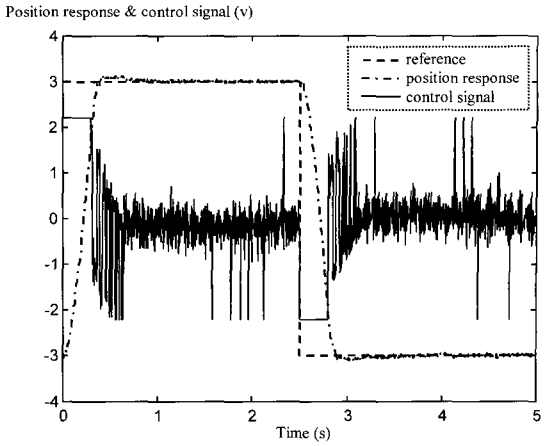

Fig. 10. Position response and control signal after incorporating lag compensator.

After incorporating the designed lag compensator, the original lead compensator turns into a lead-lag compensator. It must be pointed out that the established procedures for designing lead compensator are still valid, because there is almost no interference between the original lead compensator and the added lag compensator.

Fig. 10 shows the experimental system response and the actual control signal after adding the designed lag compensator. It can be seen that the control chattering caused by noises are greatly reduced while the system response remains very similar to the one without a lag compensator.

6. CONCLUSION

This paper proposes a Concurrent Relay-PID controller (CRPID) for motor position servo systems. The proposed controller is composed of a deadband-relay subcontroller and a parallel PID subcontroller. The deadband-relay subcontroller improves the transient system performance while the PID subcontroller is mainly responsible for the steady-state system performance. A very promising advantage of this hybrid scheme, in terms of controller synthesis, is that the subcontrollers and controller components may be designed separately. Both numerical and experimental results have demonstrated the effectiveness of the proposed controller and its superiority over PID control.

Although the paper focused on the discussion of the approach with reference to a motor position servo system, the proposed method can actually be extended to a wider range of different applications. This is because the developed approach did not depend on any specific nature(s) of motor servo systems.

REFERENCES

[1] A. A. EI-Samahy, M. A. EI-Sharkawi, and S. M.

Sharaf, "Adaptive multi-layer self-tuning high performance tracking control for DC brushless motors," *IEEE Trans. on Energy Conversion*, vol. 9, pp. 311-316, 1994.

[2] W. J. Wang and C. C. Wang, "A rotor flux observer based composite adaptive speed controller for an induction motor," *IEEE Trans. on Energy Conversion*, vol. 12, pp. 323-329, 1997.

[3] J. Y. Hung, R. M. Nelms, and P. B. Stevenson, "An output feedback sliding mode speed regulator for dc drives," *IEEE Trans. Ind. App.*, vol. 30, pp. 691-698, 1994.

[4] F. F. Cheng and S. N. Yeh, "Application of fuzzy logic in the speed control of AC servo system and an intelligent inverter," *IEEE Trans. on Energy Conversion*, vol. 8, pp. 312-318, 1993.

[5] P. K. Nandam and P. C. Sen, "Analog and digital speed control of dc drives using proportional-integral and integral-proportional control techniques," *IEEE Trans. Ind. Electron*, vol. 34, pp. 227-233, 1987.

[6] S. Ogasawara and H. Akagi, "Implementation and position control performance of a position sensorless IPM motor drive system based on magnetic saliency," *IEEE Trans. Ind. App.*, vol. 34, pp. 806-812, 1998.

[7] J. H. Kim, K. C. Kim, and E. K. P. Chong, "Fuzzy precompensated PID controllers," *IEEE Trans. Contr. Sys. Tech.*, vol. 2, pp. 406-411, 1994.

[8] N. Matsunaga, "Fuzzy hybrid control of DC servomotor," *Trans. IEE Japan*, vol. 111, pp. 105-111, 1991.

[9] G. Li, K. M. Tsang, and H. Li, "Concurrent FL-PI controller designed using Gas," *Proc. of the 34th Annual Allerton Conference on Communication, Control and Computing*, Champaign-Urbana, USA, pp. 942-949, Oct. 2-4, 1996.

[10] Y. Z. Tsypkin, *Relay Control Systems*, University Press, Cambridge, UK, 1984.

[11] K. J. Astrom and T. Hagglund, *Automatic Tuning of PID Regulators*, Instrument Society of America, Research Triangle Park, NC, 1988.

[12] G. Li, *Robust Control Strategies for Motor Servo Systems*, Ph.D. Thesis, The Hong Kong Polytechnic University, Hong Kong, 1999.

[13] K. M. Tsang and G. Li, "Robust nonlinear nominal model following control to overcome deadzone nonlinearities," *IEEE Trans. Ind. Electron*, vol. 48, pp. 177-184, 2001.

[14] J. G. Ziegler and N. B. Nichols, "Optimum settings for automatic controllers," *Trans. ASME*, vol. 64, pp. 759-768, 1942.

[15] K. Ogata, *Modern Control Engineering*, 2nd ed., Prentice Hall, Englewood Cliffs, New Jersey, 1990.

Guomin Li received the B.Sc., M.A.Sc., and Ph.D. degrees, all in Electrical Engineering, from Wuhan Institute of Technology, Beijing Institute of Technology, and Hong Kong Polytechnic University, in 1983, 1988, and 1999, respectively. He ever worked in Tianjin University, Hong Kong Polytechnic University, and Ryerson University as Faculty, Senior Researcher or Post-doctoral Research Fellow, before joining Axiomatic. His research interests include control theories and applications, intelligent control, motion control, embedded systems and mechatronics, precision electrohydraulic systems, and networked vehicle control.

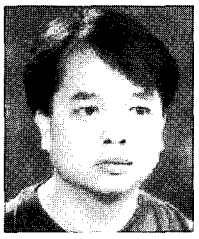

Kai Ming Tsang received the B.Eng. and Ph.D. degrees in Control Engineering from the University of Sheffield, U.K., in 1985 and 1988 respectively. At present, he is an Associate Professor in the Department of Electrical Engineering of the Hong Kong Polytechnic University. His research interests include system identification, fuzzy logic, adaptive control and pattern recognition.